52nd IEEE Conference on Decision and Control
December 10-13, 2013. Florence, Italy

LIDAR-assisted Preview Controllers Design for a MW-scale Commercial Wind Turbine Model

Na Wang, Kathryn E. Johnson, Alan D. Wright and Carlo E. Carcangiu

Abstract— **Existing commercial wind turbine control algorithms are typically feedback only. Nacelle-based commercial light detection and ranging (LIDAR) systems, which can detect preview wind information in front of the turbine to be used in feedforward controller design, can improve wind turbine control performance compared to a baseline standard proportional-integral (PI) feedback controller. Combined feedforward and feedback collective pitch control strategies are investigated in this research for both mitigating tower fore-aft fatigue load above rated wind speed and enhancing power capture below rated wind speed. When the wind speed is above rated, we consider a collective pitch LQ-based preview control scheme that augments the existing feedback controller and uses a Kalman filter in the control loop as the observer. When the wind speed is below rated, we combine a tower fore-aft feedback damping pitch controller with a feedforward controller designed through the method of Lagrange multipliers optimization. Control effectiveness verifications are conducted through FAST simulations with multiple turbulent wind cases.**

I. Introduction

Modern commercial wind turbine control algorithms are typically feedback only and operate on an input signal such as the error in rotor/generator speed or power. Classical PI controllers are typically used in the industry for blade pitch and generator torque controllers to regulate turbine speed with varying wind conditions. Recent advances in LIDAR systems have shown promise for providing real-time measurements of wind speed or direction inputs local to wind turbines [1], [2], giving a new area of research in feedforward wind turbine control. Nacelle- or hub-based LIDAR systems have been investigated in [3], [4], [5]. The improvement of speed regulation and fatigue load reduction can be achieved via a look-ahead update to the collective pitch control. As presented in [6], assuming both a highly idealized wind measurement and a more realistic LIDAR model, preview control-based disturbance feedforward controllers designed with and without the use of multi-blade coordinate (MBC) show excellent performance in load mitigation. The application of LIDAR plus model predictive control (MPC) for wind turbines can be found in [7], [8] for the fatigue load and extreme load reduction over the full operation regime. An extreme event controller designed to prevent rotor overspeed in response to incoming wind gusts can be found in [9], where LIDAR is used in conjunction with a Cumulative Summation (CUSUM) test to detect an oncoming gust. Baseline feedback controllers augmented with various collective/individual pitch feedforward controllers have been investigated in other LIDAR-enabled control research [10], [11], [12], including the use of model-inverse and shaped compensators, or adaptive FIR feedforward controller.

In this paper, efforts are focused on augmenting the baseline pitch controller using a LQ-based preview collective pitch controller for tower fore-aft fatigue load mitigation above rated wind speed. The work described in this paper differs from other above-rated LIDAR-enabled preview control strategies in that it augments instead of replaces an existing feedback controller and also by using a Kalman filter as an observer in the preview controller. That is, there would be two feedback control loops: one is the baseline pitch controller for speed regulation; the other is solved from the optimal preview control strategy for tower fore-aft fatigue load mitigation. Also, the baseline controller can provide anti-windup compensation.

In below-rated conditions, most control strategies use generator torque to optimize the power coefficient (C_p) based on the power or speed error, while the blades are kept at the constant pitch values corresponding to the maximum aerodynamic efficiency [13], [14]. LIDAR-assisted optimal C_p tracking control are investigated in [15], but the benefits over conventional methods are less clear.

In [16], a method for yaw error estimation based on measurements from a spinner-based LIDAR is developed for improved yaw control of horizontal axis wind turbines in turbulent flow. Further field test study shown in [17] indicates that applying a correction scheme to improve yaw alignment increases the power capture by 1-5 % in the below-rated domain. In this research our novel contribution in below-rated operation is to combine a tower fore-aft feedback damping pitch controller with a feedforward controller, which is solved via the Lagrange parameter optimization technique, to improve power production below rated.

The remainder of this paper is organized as follows. Section II introduces the design of preview controllers for Region 3 where wind speed is above rated and Region 2.5 where wind speed is just below rated. Section III describes the simulated wind turbine model, turbulent wind fields and LIDAR model. Section IV gives the simulation results compared with a baseline controller. Finally, concluding

Na Wang is the Graduate Student at Colorado School of Mines, Department of Electrical Engineering and Computer Science, Golden, CO, USA. nwang@mymail.mines.edu

Kathryn E. Johnson is the Associate Professor at Colorado School of Mines, Department of Electrical Engineering and Computer Science, and Joint Appointee at National Renewable Energy Laboratory's National Wind Technology Center, Golden, CO, USA. kjohnson@mines.edu

Alan D. Wright is the Principal Engineer at National Renewable Energy Laboratory, Golden, CO, USA. alan.wright@nrel.gov

Carlo E. Carcangiu is the Head of Closed-Loop Control at ALSTOM WIND S.L.U., Barcelona, Spain. carlo-enrico.carcangiu@power.alstom.com

978-1-4673-5716-6/13/$31.00 ©2013 IEEE

remarks are given in Section V.

II. LIDAR-Assisted Preview Controllers Design

Two preview controllers are designed for Region 3 and Region 2.5. The preview control scheme for Region 3 is based on a LQ-based methodology from Hac [18] and the one for Region 2.5 is solved using the Lagrange parameter optimization technique from Tomizuka [19].

A. Controller Design for Region 3

Preview control is a technique for synthesizing closed-loop control of linear time-invariant (LTI) systems during tracking of previewed inputs by minimizing a defined output error. Using National Renewable Energy Laboratory (NREL)'s FAST linearization routine [20], a discrete-time linearized turbine model for pitch control design in this research can be obtained, and is given by

$$\begin{aligned} \Delta w(n+1) &= \Lambda \Delta w(n) + \Gamma \Delta \beta_c(n) + \Upsilon \Delta u(n), \\ \Delta \Omega(n) &= H_{RS} \Delta w(n), \end{aligned} \tag{1}$$

where $\Lambda, \Gamma, \Upsilon, H_{RS}$ are discrete-time state space model matrices; w contains the plant states, including

$$w = \begin{bmatrix} \text{Tower fore-aft deflection (m)} \\ \text{Tower fore-aft velocity (m/s)} \\ \text{Rotor speed (m/s)} \end{bmatrix}; \tag{2}$$

β_c is the blade pitch command; Ω is the rotor speed; u is the wind speed disturbance; and deviations from the operating points are described with Δ. The operating point is selected at a wind speed u_0 = 15 m/s.

As shown in Fig. 1, the preview control is configured to augment a PI collective pitch control (baseline pitch control). A Kalman filter using rotor speed measurement and nacelle inertial measurement unit (IMU) velocity in the vector $\Delta\psi$ is designed for state estimation. The noise levels for the rotor speed measurement, IMU velocity measurement and process are 10, 10, and 10, respectively. Also, $\Delta\phi$ is the generator speed measurement used by the baseline pitch controller, Δx is the LIDAR measurement, and $\Delta\beta_c$ is the combined pitch command obtained from the preview controller ($\Delta\beta_P$) and the baseline controller ($\Delta\beta_{BS}$).

The augmented turbine plant model constructed by augmenting (1) with the baseline PI controller is formulated as

$$\begin{aligned} \Delta \bar{w}(n+1) &= \bar{\Lambda} \Delta \bar{w}(n) + \bar{\Gamma} \Delta \beta_P(n) + \bar{\Upsilon} \Delta u(n), \\ \Delta \psi(n) &= \bar{H}_{\{\cdot\}} \Delta \bar{w}(n), \end{aligned} \tag{3}$$

where $\Delta\bar{w}$, $\bar{\Lambda}$, $\bar{\Gamma}$ and $\bar{\Upsilon}$ are given by

$$\begin{aligned} \Delta \bar{w} &= \begin{bmatrix} \Delta w \\ \Delta \xi \end{bmatrix} \\ \bar{\Lambda} &= \begin{bmatrix} \Lambda + \Gamma G_{wBS} & \Gamma G_{\xi BS} \\ H_{RS}\Lambda + H_{RS}\Gamma G_{wBS} & I + H_{RS}\Gamma G_{\xi BS} \end{bmatrix} \\ \bar{\Gamma} &= \begin{bmatrix} \Gamma \\ H_{RS}\Gamma \end{bmatrix} \\ \bar{\Upsilon} &= \begin{bmatrix} \Upsilon \\ H_{RS}\Upsilon \end{bmatrix} \\ \bar{H}_{\{\cdot\}} &= \begin{bmatrix} H_{\{\cdot\}} & 0 \end{bmatrix}. \end{aligned} \tag{4}$$

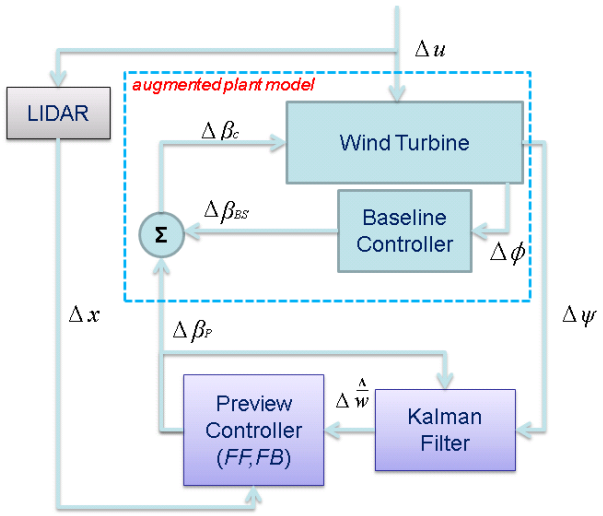

Fig. 1. Preview controller designed with Kalman filter for Region 3 control. The preview controller contains a feedforward term and a feedback term. The feedforward term is based on the previewed measurement from a LIDAR system, and the feedback term is based on the Kalman filter output. The wind turbine model is augmented by the baseline pitch controller.

In (4), I is the identity matrix with appropriate size and the subscript $\{\cdot\}$ can be defined to select the desired output signal, e.g. $H_{NcIMUTAxs}$ is related to the IMU acceleration in the fore-aft direction. The model of the baseline PI controller can be expressed by

$$\begin{aligned} \Delta\beta_{BS}(n) &= (k_p + k_i \frac{q}{q-1} \cdot \delta) e(n) \\ &= G_{wBS} \Delta w(n) + G_{\xi BS} \Delta \xi(n), \end{aligned} \tag{5}$$

where q is the forward shift operator; δ is the sampling time; e is the generator speed error; $\Delta\xi$ is an additional state related to the integral of rotor speed error; k_p and k_i are proportional and integral gains; and G_{wBS} and $G_{\xi BS}$ are gains associated with states Δw and $\Delta\xi$, respectively.

The preview control strategy combines the design of the controller including feedback and feedforward terms so that the cost J is minimized in the presence of the exogenous input [18], [21]. The cost function J is given by

$$\begin{aligned} \min J = E\Big\{ & \frac{1}{2} \Delta \bar{w}(\infty)^T S \Delta \bar{w}(\infty) + \\ & \frac{1}{2} \int_0^\infty [\Delta \bar{w}(t)^T Q \Delta \bar{w}(t) + \Delta \beta_P(t)^T R \Delta \beta_P(t)] dt \Big\}, \end{aligned} \tag{6}$$

where $E\{\cdot\}$ is the expression for expected value, and S, Q, and R are the weighings associated with plant state vector and blade pitch control authority. Q can be chosen as

$$Q = \bar{H}_{NcIMUTAxs}^T \bar{H}_{NcIMUTAxs} \tag{7}$$

to minimize the IMU acceleration in the fore-aft direction for the purpose of tower fore-aft load mitigation, and $R = 500$ is selected after considering both tower base fore-aft bending moment and low-speed shaft load via several simulation

tests. The entire preview control law including both feedback and feedforward terms is given by

$$\Delta\beta_P(n) = G_w\Delta\hat{\bar{w}}(n) + \sum_{j=0}^{h} G_u\Delta u(n+j), \tag{8}$$

where G_w and G_u are the feedback and feedforward gains in the preview controller and u can be measured by the LIDAR sensor; that is, $x(n+1) = u(n+h)$, where x is the LIDAR measurement shown in Fig. 1 and h is the number of discrete time steps used in preview. The plant state vector $\Delta\hat{\bar{w}}$ is obtained from the Kalman filter. According to [18], stability of the linear-based preview controller is guaranteed by finding the positive definite symmetric solution of an algebraic Riccati equation (ARE). The Kalman filter is independent of the control since the separation principle holds.

B. Controller Design for Region 2.5

When the wind speed is below rated, we can further divide it into two regions: Region 2 and Region 2.5. In Region 2, both generator torque and generator/rotor speed are below their rated values. Therefore, a standard generator torque controller is designed to optimize the power coefficient C_p and the blade pitch angle is held constant giving the maximum aerodynamic efficiency as shown in [13]. Region 2.5 is a transition region between Region 2 and Region 3 and its specifics vary for individual turbines. Tip-speed ratio (TSR) is defined as

$$\lambda = \frac{\Omega}{u}R, \tag{9}$$

where Ω is the rotor speed, u is the wind speed, and R is the rotor radius. Due to a higher optimal TSR, the rotor speed of the turbine used in this research reaches its rated value below rated wind speed (in Region 2.5). Thus, the TSR decreases in Region 2.5 to keep the rotor speed at its rated value; that is, the turbine operates away from the peak C_p value.

The reduced C_p due to decreased TSR can be mitigated by varying the pitch angle setpoint according to a look-up table based on the turbine's C_p vs. TSR and pitch surface. The optimal setpoints are shown as black triangle markers in Fig. 2, where the baseline (constant) pitch angle for Region 2 is given by the blue solid line. However, using the static pitch angles indicated by the black triangles can worsen the tower fore-aft loads despite improving energy capture. Therefore, controlling based on optimal pitch setpoint in Region 2.5 is undesirable. In this research, we consider both a feedback-only tower fore-aft damping collective pitch controller ('R2.5-TwrFAD-Control') and a feedforward pitch controller augmenting this predetermined feedback control ('R2.5-Preview-Control'). Both controllers also contain the baseline PI torque controller in the control loop to regulate the rotor speed at its rated value. 'R2.5-TwrFAD-Control', which is based on the 1st tower fore-aft velocity measurement (v_{TFA}), helps to alleviate the tower fore-aft fatigue damage. The tower fore-aft damping control can be expressed by

$$\Delta\beta_{TD} = K_{TD}v_{TFA}, \tag{10}$$

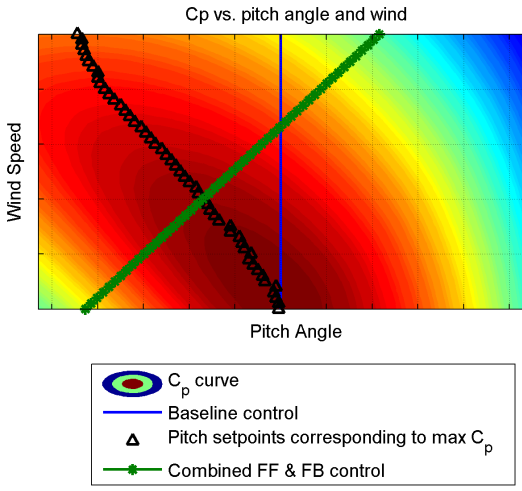

Fig. 2. C_p surface versus wind speed and pitch angle for a 3 MW turbine investigated in this research. The constant pitch strategy is indicated by the blue solid line, while the preview control-based pitch control in Region 2.5 is designated by the green star markers. The pitch setpoints corresponding to the max C_p are indicated by the black triangle markers. The wind speeds shown range across Region 2.5, and the rotor speed reaches rated in this region. Axis values have been removed to protect intellectual property.

where v_{TFA} can be obtained by integrating of IMU acceleration in the fore-aft direction and K_{TD} is the feedback control gain. By several experimental trials, is selected as 0.05 $(rad \cdot s/m)$ in this paper.

To design the 'R2.5-Preview-Control', the Region 2.5 optimization problem, also based on (6), is designed to minimize the 1st tower fore-aft motion without significantly increasing the pitch control authority. We keep the same basic structure as (1) and (3), except that since operation is in Region 2.5 we replace β_c with τ as the control input to augment the baseline torque control. Also, the state vector w is now

$$w = \begin{bmatrix} \text{Tower fore-aft deflection [m]} \\ \text{Tower side-to-side deflection [m]} \\ \text{Tower fore-aft velocity [m/s]} \\ \text{Tower side-to-side velocity [m/s]} \\ \text{Rotor speed [m/s]} \end{bmatrix} \tag{11}$$

instead of (2). As described in [19], the feedforward control in 'R2.5-Preview-Control' is constructed by the solution P for the Lyapunov equation

$$\begin{aligned} \bar{\bar{\Lambda}}^T P\bar{\bar{\Lambda}} - P + Q = 0, \\ \bar{\bar{\Lambda}} = \bar{\Lambda} + \bar{\Gamma}[0, 0, K_{TD}, 0, 0], \end{aligned} \tag{12}$$

where $\bar{\bar{\Lambda}}$ is the eigenmatrix formed by augmenting $\bar{\Lambda}$ with predetermined 'R2.5-TwrFAD-Control', Q is the weight designed to mitigate the 1st tower fore-aft motion, and P can be solved by a Lagrange parameter optimization technique indicated in [19]. The operating point is selected at a wind speed of 9 m/s.

Adding the feedforward control constructed via (12) to the optimal pitch setpoint given by the black triangles in Fig. 2 results in a pitch schedule given by the green star markers. Due to the fact that the feedforward control tries to mitigate tower fore-aft bending moment, the pitch angles are increasing with the increase in wind speed. This new pitch scheduling controller makes the turbine operate in an improved C_p compared to the non-pitch control (blue solid line) around the selected operating point (the intersection of black and green markers). However, when operating away from the operating point, the feedforward controller would

degrade the aerodynamic efficiency. Thus, a trade-off has been made to increase energy without increasing tower fore-aft bending moment. In summary, the Region 2.5 control diagram is shown in Fig. 3, where the optimal pitch setpoint strategy is determined from the balance between energy and loads according to the green star markers in Fig. 2.

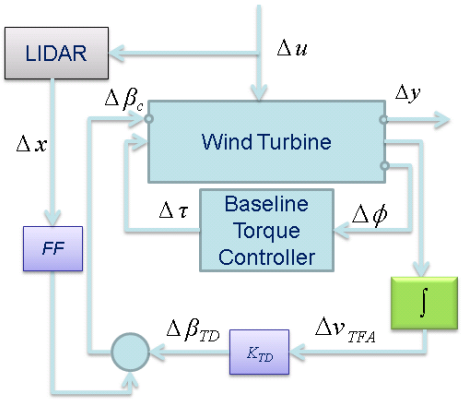

Fig. 3. Region 2.5 control diagram. The feedforward controller (FF) and the tower fore-aft feedback damping controller (K_{TD}) are combined via a preview controller design process. The baseline torque control is held in the control loop to regulate rotor speed.

The magnitude Bode plots of the closed loop transfer functions resulting from the Fig. 3 configuration are shown in Fig. 4. The input is the wind disturbance Δu and the outputs Δy is the tower fore-aft bending moment error. It is seen that compared with the non-pitch control in Region 2.5 (blue solid line), 'R2.5-TwrFAD-Control' (green dotted line) helps to alleviate the 1st tower fore-aft magnitude at the tower mode and 'R2.5-Preview-Control' (red dash-dotted line) further reduces the tower loads across a wider range of frequencies.

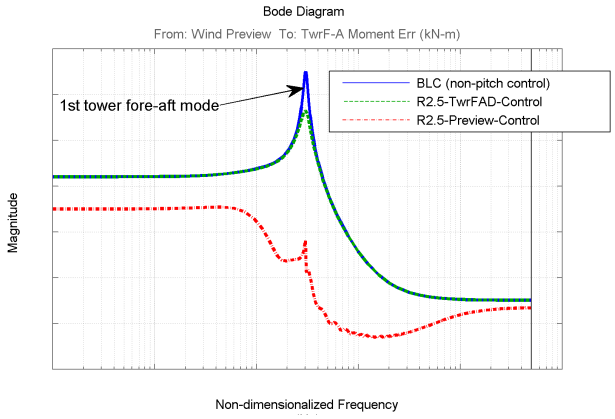

Fig. 4. Bode magnitude plots of the closed loop for Region 2.5 with the controllers described in Section II.B.

III. Simulated Turbine Model, Turbulent Wind Fields and LIDAR Model

The utility-scale turbine used in this research is the Alstom ECO-100, a 3 MW upwind horizontal-axis commercial turbine equipped with three blades, variable pitch and variable speed and with maximum pitch rate 5 deg/s. FAST [20] is used to model the turbine associated with the generator mode (1 DOF), drivetrain mode (1 DOF), first and second blade flapwise modes (2×3 DOFs), first blade edgewise mode (1×3 DOFs), first and second tower fore-aft modes (2 DOFs), first and second tower side-to-side modes (2 DOFs) and Yaw mode (1 DOF). A second order pitch actuator model is implemented in this research.

A series of TurbSim-generated [22] wind input files are used as turbulent wind fields for the simulations carried out in this research. TurbSim uses a statistical model to numerically simulate the time series of three component wind speed vectors at points in a two-dimensional vertical rectangular grid.

A continuous wave (CW) coherent Doppler LIDAR system mounted on the back of turbine nacelle is considered in this research. Three stationary preview measurements are obtained by the LIDAR simulator presented in [23]. The TurbSim-generated wind fields shown in Fig. 5 march forward to the rotor plane without evolution. The LIDAR system measures the wind speed within specified cylindrical volumes along each of three beams that are aimed so that the volume centers are located at a distance of 75% of the blade radius from the hub and about 1.2 rotor diameters in front of the turbine. The space weighting function provides a weighted average of velocities within the specified volume with velocities at locations close to the focal location contributing most to the computed velocity [24]. The general effect of distance weighting is low-pass filtering (LPF) of the wind speed with respect to space.

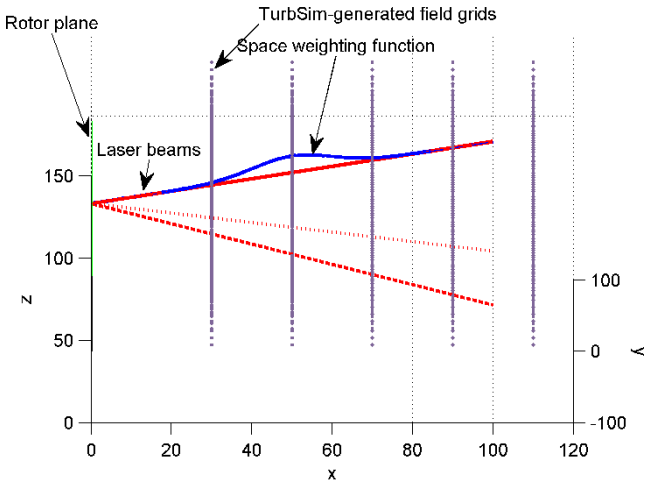

Fig. 5. Schematic diagram showing the 3-beam LIDAR configuration and the TurbSim-generated wind fields. The LIDAR is mounted on the turbine's nacelle and focuses its three stationary beams at 75% of blade span 1.2 rotor diameters upwind of the turbine. x refers to the prevailing direction, y refers to the direction perpendicular to x but parallel to the ground, and z refers the vertical direction. The TurSim-generated field grids are 20 Hz, and only five sample grids are shown.

These LIDAR measurements have been incorporated in the FAST turbine dynamics code [25]. By setting the preview time for the wind speed measurement, the mean wind speed, and the update rate in the simulation, the CW LIDAR model can provide wind measurements at the desired distance in front of the turbine. The LIDAR measurements are filtered using a moving average corresponding to the preview time to smooth out high frequency wind fluctuations.

IV. Simulation Results and Discussion

In this section, the performance of the control strategies proposed in Section II are quantified using the non-linear turbine model described in Section III.

A. Performance for Region 3 LQ-based Preview Controller with BLC

Thirty TurbSim-generated IEC Kaimal spectral model turbulent wind files with mean wind speeds of 15 m/s and average turbulence

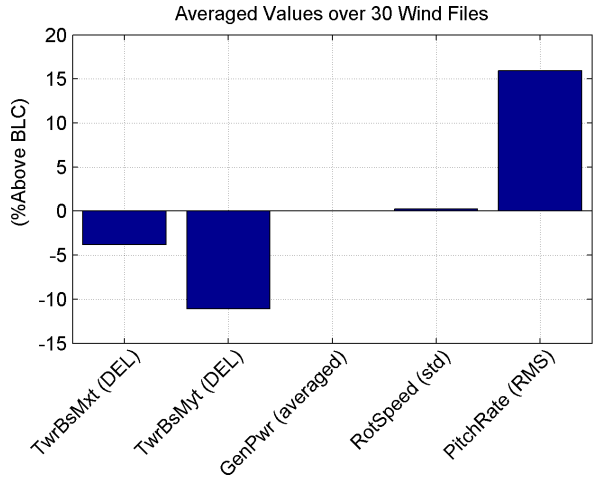

Fig. 6. Comparison of DELs between the Region 3 preview control and the baseline PI control: DELs values of tower base fore-aft/side-to-side bending moment, averaged generator power, std of rotor speed, and RMS value of pitch rate.

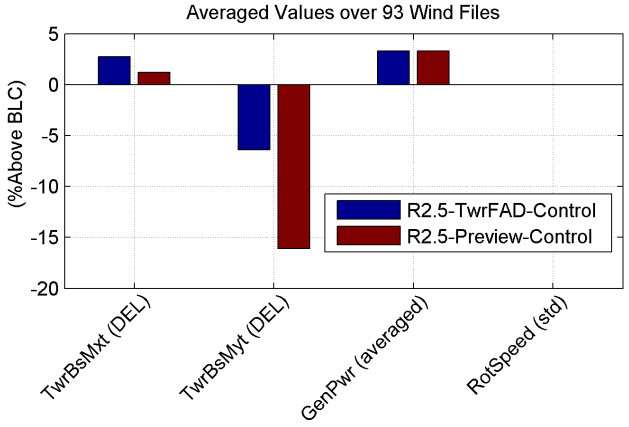

Fig. 7. Comparison of DELs between the Region 2.5 preview controllers with the baseline non-pitch control: DELs values of tower base fore-aft/side-to-side bending moment, averaged generator power, and std of rotor speed.

intensities of 16% are used to test the Region 3 preview controller. Controller effectiveness is based on damage equivalent loads (DELs) using a rainflow counting algorithm presented in [26]. We examine DELs of tower base fore-aft and side-to-side bending moment (TwrBsMyt and TwrBsMxt, respectively), averaged generator power, standard deviation (std) of rotor speed, and root mean square (RMS) value of pitch rate. As show in Fig. 6, the Region 3 preview control decreases the tower fore-aft DELs by over 10% without diminishing the generator power production and rotor speed, and increases the RMS pitch rate by 15% due to the additional pitch activity. Although better percent reductions appear in the literature (e.g., [4]), it is difficult to make a direct comparison since the turbine and baseline controller are different from that paper.

B. Performance for Region 2.5 Controllers

The performances of the two Region 2.5 controllers are verified with 93 TurbSim-generated wind files with mean wind speeds of 9 m/s and average turbulence intensities of 7%; the low turbulence is required to ensure operation within Region 2.5, since there is no controller transition strategy included in the implementation. Control effectiveness is based on tower base fore-aft and side-to-side DELs and averaged generator power. As shown in Fig. 7, the average generator power has been increased using either 'R2.5-TwrFAD-Control' or 'R2.5-Preview-Control' by up to 3%. This increase is because the generator torques in both controllers are increased with the rated rotor speed regulation and the pitch actuations around the operating point. 'R2.5-TwrFAD-Control' decreases the tower base fore-aft DELs at the tower mode and 'R2.5-Preview-Control' further mitigates the tower fore-aft DELs up to 15%. Rotor speed is similar to the baseline using both controllers. Also, tower base side-to-side DELs are increased by 2.5% or so, which might be caused by increased generator torque control actuation for speed regulation after introducing the pitch control in Region 2.5. A 30% increase in averaged absloute value of pitch rate (not shown) was seen in 'R2.5-Preview-Control' compared to 'R2.5-TwrFAD-Control' due to extra pitch activity from the feedforward control.

In Fig. 8, the tower base fore-aft bending moment versus wind speed plot and power spectral density (PSD) plot of the tower base fore-aft bending moment are shown from one of the 93 simulation results. As shown in the subplot (a), the normalized magnitude of tower base fore-aft bending moment from the 'R2.5-TwrFAD-Control' is worse than the baseline non-pitch control within Region 2.5 (green dots vs. blue dots). This increase is caused by the move toward the optimal pitch angle for power and the associated increase in thrust coefficient (Fig. 2). And adding preview control for tower fore-aft mitigation improves this moment at higher wind speed and worsens it at lower wind speed, which is because the operating point designed for 'R2.5-Preview-Control' is selected at the middle of Region 2.5 as shown in Fig. 2. Based on the view shown in (b), 'R2.5-TwrFAD-Control' decreases the magnitude of tower fore-aft bending moment at the tower mode and the 'R2.5-Preview-Control' further attenuate the magnitude at lower frequencies.

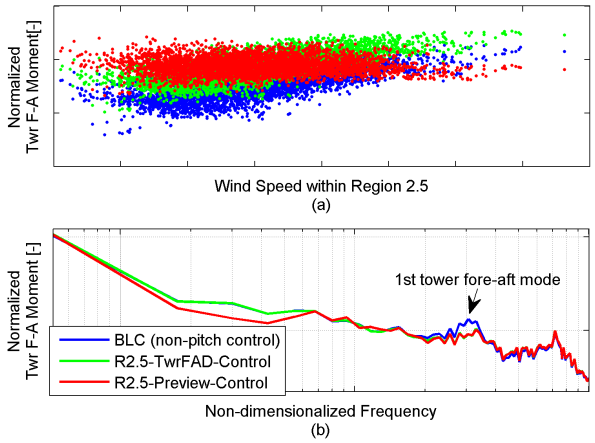

Fig. 8. Comparison of tower fore-aft bending moment between the Region 2.5 controllers with the baseline non-pitch control in moment versus speed plot and PSD plots.

V. Conclusion and Future Work

In this paper, two preview control-based combined feedforward and feedback controllers have been introduced and tested using multiple turbulent wind inputs to a non-linear FAST turbine model with a CW LIDAR system embedded in the code. The investigated controllers are designed for both mitigating tower fore-aft fatigue load above rated wind speed and enhancing power capture below rated wind speed. In above rated wind speed conditions, the LQ-based preview collective pitch control scheme, augmented with the existing PI feedback controller and using a Kalman filter, have been considered. We achieved more than 10% reduction in the

tower base fore-aft DELs without diminishing the generator power production and rotor speed regulation, although pitch actuator usage was increased.

When the wind speed is below rated, a Lagrange multipliers optimization based feedforward control, combined with the pre-determined tower fore-aft feedback damping pitch controller, has been investigated. Using only a modification to the pitch control setpoint in Region 2.5 results in the averaged generator power being increased by 3% in those 93 lower turbulent intensity wind files. Using the feedforward controller obtained from the Lagrange multipliers optimization further reduces the tower base fore-aft bending moment DELs up to 15%.

Overall, the preview control-based combined feedforward and feedback control strategies presented in this paper show promising results for the 3 MW commercial turbine in both above and below rated wind speed conditions for tower fore-aft fatigue load mitigation and power production enhancement. Although a LIDAR system that can provide the required preview information in front of the turbine enables these novel controllers, a further study should be conducted to assess the sensitivity of the controllers to measurement uncertainty. Future work will also include the gain scheduling of those linear control strategies and considering additional wind input files that more fully encompass the range of operating conditions.

ACKNOWLEDGMENTS

The presented work was supported by the U.S. Department of Energy through grant no. DE-EE0005494. The authors would also like to thank Paul Fleming from the U.S. National Renewable Energy Laboratory for his assistance in this research.

REFERENCES

[1] M. Harris, S. M. Hand, and A. Wright, *Lidar for Turbine Control*. Golden, CO: National Renewable Energy Laboratory, Jan. 2006.

[2] T. Mikkelsen, K. Hansen, N. Angelou, M. Sjöholm, M. Harris, P. Hadley, R. Scullion, and G. Ellis, "Lidar wind speed measurements from a rotating spinner," in *European Wind Energy Conference and Exhibition*, (Poland,Warsaw), April 2010.

[3] D. Schlipf and M. Kühn, "Prospects of a collective pitch control by means of predictive disturbance compensation assisted by wind speed measurements," in *German Wind Energy Conference (DEWEK)*, (Bremen,Germany), pp. 1–4, 2008.

[4] D. Schlipf, T. Fischer, C. E. Carcangiu, M. Rossetti, and E. Bossanyi, "Load analysis of look-ahead collective pitch control using lidar," in *German Wind Energy Conference (DEWEK)*, (Bremen,Germany), pp. 1–4, 2010.

[5] D. Schlipf, S. Schuler, P. Grau, F. Allgöwer, and M. Kühn, "Look-ahead cyclic pitch control using lidar," in *TORQUE 2010, Third Conference*, (Greece), pp. 1–7, June 28-30 2010.

[6] J. Laks, L. Y. Pao, A. Wright, N. Kelley, and B. Jonkman, "Blade pitch control with preview wind measurements," in *Proc. 48th AIAA Aerospace Sciences Meeting Including the New Horizons Forum and Aerospace Exposition*, 2010.

[7] J. Laks, L. Y. Pao, A. Wright, N. Kelley, and B. Jonkman, "Model predictive control using preview measurements from lidar," in *Proc. 49th AIAA Aerospace Sciences Meeting Including the New Horizons Forum and Aerospace Exposition*, 2011.

[8] D. Schlipf, D. Schlipf, and M. Kühn, "Nonlinear model predictive control of wind turbines using lidar," in *Wind power conference and exhibition*, (Anaheim,CA), pp. 1–18, American Wind Energy Association, May 2011.

[9] A. Pace and K. E. Johnson, "Lidar-based extreme event control to prevent wind turbine overspeed," in *Proc. 50th AIAA Aerospace Sciences Meeting Including the New Horizons Forum and Aerospace Exposition*, 2012.

[10] F. Dunne, L. Y. Pao, A. D. Wright, B. Jonkman, and N. Kelley, "Combining standard feedback controllers with feedforward blade pitch control for load mitigation in wind turbines," in *Proceedings of American Institute of Aeronautics and Astronautics*, 2010.

[11] N. Wang, K. E. Johnson, and A. D. Wright, "FX-RLS-Based Feedforward Control for LIDAR-Enabled Wind Turbine Load Mitigation," in *IEEE Transactions on Control Systems Technology*, pp. 1–11, 2011.

[12] N. Wang, K. E. Johnson, and A. D. Wright, "Pulsed lidar-enabled torque controller design for turbine power capture enhancement and fatigue loads mitigation," in *review for IEEE Transactions on Control Systems Technology's upcoming special issue To tame the wind: advanced control applications in wind energy*, 2011.

[13] K. E. Johnson, L. Y. Pao, M. J. Balas, and L. J. Fingersh, "Control of variable-speed wind turbines: Standard and adaptive techniques for maximizing energy capture," *IEEE Control Systems Magazine*, vol. 26, pp. 70–81, June 2006.

[14] M. J. Balas, Y. J. Lee, and L. Kendall, "Disturbance tracking control theory with application to horizontal axis wind turbines," in *Proc. 17th ASME Wind Energy Symposium*, (Reno, NV), 1998.

[15] N. Wang, K. E. Johnson, and A. D. Wright, "Pulsed lidar-assisted controllers for turbine power capture enhancement and fatigue load mitigation below rated," in *Proc. 50th AIAA Aerospa ce Sciences Meeting*, (Nashville, Tennessee), pp. 1–11, 09-12 January 2012.

[16] K. A. Kragh, M. H. Hansen, and T. Mikkelsen, "Improving yaw alignment using spinner based lidar," in *49th AIAA Aerospace Sciences Meeting Including the New Horizons Forum and Aerospace Exposition*, (Orlando,Florida), Jan 2011.

[17] K. A. Kragh and P. A. Fleming, "Rotor speed dependent yaw control of wind turbines based on empirical data," in *50th AIAA Aerospace Sciences Meeting Including the New Horizons Forum and Aerospace Exposition*, (Nashville, Tennessee), Jan 2012.

[18] A. Hać, "Optimal linear preview control of active vehicle suspension," in *Proc. of the 29th Conference on Decision and Control*, (Honolulu, Hawaii, USA), Decembe r1990.

[19] M. Tomizuka and D. Fung, "Design of digital feedforward/preview controller for processes with predetermined feedback controller," in *Transactions of ASME Journal*, vol. 102, pp. 218–225, Dec. 1980.

[20] J. M. Jonkman and M. L. Buhl, *FAST User's Guide*. Golden, CO: National Renewable Energy Laboratory, 2005.

[21] K. Takaba, "A tutorial on preview control systems," in *Proc. SICE Annual Conference*, (Fukui University,Japan), August 2003.

[22] N. D. Kelley and B. J. Jonkman, *Overview of the Turbsim Stochastic Inflow Turbulence Simulator: Version 1.21 (Revised Feb. 1, 2007)*. Golden, CO: National Renewable Energy Laboratory, April 2007.

[23] E. Simley, L. Y. Pao, R. Frehlich, B. Jonkman, and N. Kelley, "Analysis of wind speed measurements using coherent lidar for wind preview control," in *Proceedings of American Institute of Aeronautics and Astronautics*, 2011.

[24] M. Sjöholm, T. Mikkelsen, J. Mann, K. Enevoldsen, and M. Courtney, "Time series analysis of continuous-wave coherent doppler lidar wind measurements," in *14th International Symposium for the Advancement of Boundary Layer Remote Sensing*, pp. 1–7, 2008.

[25] F. Dunne, E. Simley, and L. Pao, *LIDAR Wind Speed Measurement Analysis and Feed-Forward Blade Pitch Control for Load Mitigation in Wind Turbines*. Golden, CO: National Renewable Energy Laboratory, 2011.

[26] S. D. Downing and D. F. Socie, "Simple rainflow counting algorithms," in *Journal of Communication and Computer*, vol. 4, pp. 31–40, Jan 1982.